

A Comparison between Estimated Shear Wave Velocity and Elastic Modulus by Empirical Equations and that of Laboratory Measurements at Reservoir Pressure Condition

Haleh Azizia^{1*}, Hamid Reza Siahkoochi², Brian Evans³,
Nasser Keshavarz Farajkhah⁴ and Ezatollah KazemZadeh⁴

¹PhD candidate, Department of Geophysics, Science and Research Branch, Islamic Azad University, Tehran, Iran

²Institute of Geophysics, University of Tehran, Tehran, Iran

³Department of Petroleum Engineering, Curtin University, Perth, Australia

⁴Research Institute of Petroleum Industry, Tehran, Iran

Received March 20, 2017; Accepted April 25, 2017

Abstract: The objective of this study is to assess the accuracy of the empirical equations in estimating the shear wave velocity and elastic modulus of rock sample at reservoir pressure condition. The evaluated relations are Gassman, Greenberg and Castagna which have been in use by researchers for a long time and have shown acceptable results. The plug sample investigated in this study is taken from Berea sandstone reservoir southwest of Australia, which is a known reference sandstone for this type of study. This plug in the laboratory was flooded with supercritical carbon dioxide fluid, saturated and pressured under axial, radial and pore pressure comparable to oil reservoirs pressures, after which elastic wave velocity and elasticity modules were determined. Then, using empirical relationships such as Gassman, Greenberg and Castagna and measured values of P-wave velocity, shear wave velocity, and elasticity coefficients were estimated. Comparison of theoretical values versus experimental values shows they compare very well, only in some cases a difference between estimated and experimental values for the coefficients of elasticity has been observed. We believe that the difference is due to the assumptions that were made in those theories. The shear wave modulus didn't remain constant during fluid saturation. Also, the measured bulk modulus and the calculated values

*Corresponding author: azizihaleh@yahoo.com

DOI: 10.7569/JSEE.2017.629502

based on Gassman formula did not compare very well. This difference was observed to be larger at higher pressures.

Keywords: Wave velocity estimate, elastic waves, the coefficients of elasticity, rock physics, reservoir conditions, Gassman relations, Greenberg – Castagna theory, injecting carbon dioxide, sandstone

1 Introduction

Study of propagation of shear and compressional waves give useful information and constitutional characteristics of hydrocarbon reservoirs, such as lithology and pore fluid type. This information is very important for reservoir development and recovery, and especially for future decision making. On the other hand, the behavior of reservoir rocks geomechanics, play an important role in the design and implementation of drilling, production planning and sustainability of oil and gas wells.

Having physical geology information such as density, porosity, compressional and shear wave velocities are required to successfully perform the above-mentioned projects. This is usually the case that the information about shear wave velocity is not readily available compared with other data. Therefore, theoretical or experimental approaches are necessary to estimate this velocity.

In geomechanical evaluation of hydrocarbon reservoirs, several methods can be used to estimate shear wave velocity and elastic constants. Conventional methods for estimating the shear wave velocity can be divided into five categories which are (Engel and Bashford, 2015; Jang *et al.*, 2015; Heureux and Long, 2016): laboratory measurements, direct measurements, empirical relationships, the regression method and the intelligent method (Figure 1).

Each of these methods has its own unique advantages that make it suitable to estimate the shear wave velocity. The dependency of wave propagation velocity to

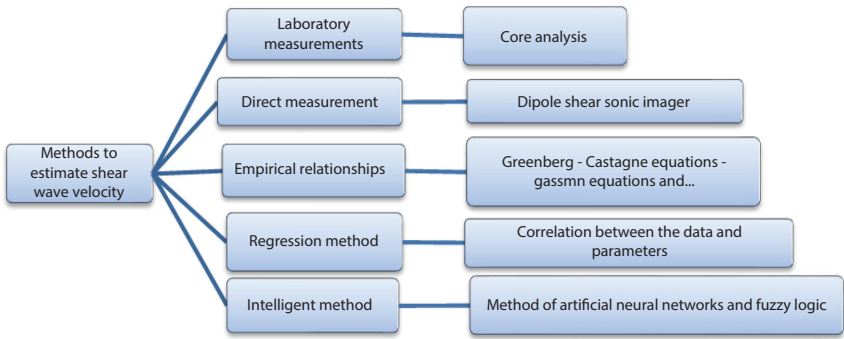


Figure 1 Common methods for estimating the shear wave velocity.

lithology, porosity, temperature, pressure and type of pore fluid, has introduced a variety of investigation methods in geophysics and rock physics.

Laboratory measurement of shear wave velocity in a core is known as a standard procedure and the obtained velocities are comparable with that of the other methods. There are other field methods to estimate shear wave velocity such as Dipole Shear Sonic Imager and sonic logs. Although these methods are common, they must be performed in a large number of wells to obtain the velocity distribution in the entire field, and core extraction or running of sonic tools in a large field is very expensive (Widarsono and Wong, 2001). Another common method to estimate the shear wave velocity is based on theoretical evaluation and modeling. In the past few decades, several empirical formulas have been introduced for estimating the shear wave velocity in rocks with different lithology, based on physical parameters of rock, especially the P-wave velocity and porosity. Many scientists, including Pickett (1963), Milholand (1980), Domenico (1984), Thomsen (1986), Han (1989), Krief (1990), Castagna (1985) and Greenberg (1992) have done very useful research in this area and various relationships have been developed and presented. These relations are valid for the saturated rocks with brine.

Gassman formulas have been introduced to extend these experimental formulas to other fluids contents. In 1986, Han offered empirical regression formulas for elastic waves in laboratory condition which would estimate the speed based on porosity and clay content. In 1989, Eberhart added the pressure parameter to Han's equation for shale sand rocks. Years before, Tosaya, Nur (1982) and Castagna *et al.* (1985) presented empirical formulas for shale sand rocks based on velocity, porosity and clay parameters.

Other methods are artificial intelligence techniques such as neural networks and fuzzy logic (Rezaee *et al.* 2007, Dezfoolian, 2013, malekia *et al.*, 2014). Although their estimates are associated with less error, these methods also present a specific model for each different field, and the results from one field cannot be applied to other fields.

There are two methods to calculate the elastic coefficients. The first one is the static method (destructive) and the other one is the dynamic (non-destructive) method. In the static method, elastic parameters of rock are calculated from laboratory measurements such as the uniaxial compressive strength of cores. But in a dynamic method, assuming that rocks are elastic, the coefficients are determined from propagating shear and compressional waves in rock and measuring waves travel time, without damaging the rock (Bell, 2000).

Currently, there is no unique empirical formula or comprehensive theory that could be utilized to determine the elastic wave velocity and elastic coefficients at different environmental conditions, type of fluid and rock. In this paper, experimental data (elastic wave propagation velocity) has been gathered using a sample saturated with water and supercritical carbon dioxide at different reservoir pressure. Then while the common fluid (brine) was replaced by critical CO₂, the elastic wave velocity values were calculated using Gassman formulas and

Greenberg - Castagna empirical equations and the results were compared with direct laboratory observations.

2 Methodology

1.2 Estimating the Shear Wave Velocity

A major part of the seismic signal analysis in regards to rock physics models relates shear wave velocity to mineralogy and porosity. Rock physics analysis based on logs and cores and the relation of these to the geological model, leads to the establishment of a relationship between velocity and porosity. Formulation of the relation between rock velocity and rock properties like porosity was initiated by Gassman (1951) and revised later on by Mavko and Mukerji (1995) and Mavko *et al.* (1998). Other studies on this subject include Wyllie *et al.* (1965), Raymer *et al.* (1980), Castagna (1985), Han (1986), Raiga- Clemenceau and colleagues (1988), Eberhart (1989), and the critical porosity model of Wang and Nur (1992).

Greenberg - Castagna model is utilized in this study to estimate the shear wave velocity of a rock sample. Greenberg and Castagna (1993) presented an empirical formula for multi-mineral rocks saturated in brine:

$$V_S = \frac{1}{2} \left\{ \left[\sum_{i=1}^L X_i \sum_{j=0}^{N_i} a_{ij} V_P^j \right] + \left[\sum_{i=1}^L X_i \left(\sum_{j=0}^{N_i} a_{ij} V_P^{-j} \right)^{-1} \right]^{-1} \right\}, \quad (1)$$

$$\sum_{i=1}^L X_i = 1$$

where L is the number of lithology in the formation, X_i is the percentage of the volume of lithology, a_{ij} is regression coefficient, N_i is the degree of polynomial regression for the targeted lithology, V_p and V_s are compression and shear wave velocities (Km/s).

This formula estimates shear wave velocity using compressional wave velocity in pure unit minerals, saturated in water. Regression coefficients of the formula for four different lithologies were presented by Greenberg and Castagna (1992).

To estimate the shear wave velocity of a brine saturated rock using Greenberg - Castagna, formula, one needs to find a way to replace the existing fluid with brine as a common fluid. This work is done by utilizing Gassman relations. In fact, by brine replacement, a similar condition is assumed for the whole environment. Then the compressional wave velocity is obtained for brine saturated situation using the following formulas. Finally, the shear wave velocity is obtained from the estimated compressional wave velocity.

Replacing different types of pore fluids with brine, and keeping the rest of the physical properties of the rock (e.g. porosity) intact, the compressional wave modulus of the rock will also be changed (Dvorkin *et al.* 2004). Compressional wave modulus is expressed as a linear combination of bulk modulus and shear modulus:

$$M = K + \left(\frac{4}{3}\right)\mu \quad (2)$$

The usual process is initiated by replacing the primary fluid with a fluid with similar sets of velocities and rock densities, compared with the primary fluid. These velocities are usually obtained from logs, but sometimes they may also be the results of theoretical models. In this study, the velocity of the wave that has passed through the primary fluid (in our case, supercritical dioxide is injected into the water) is obtained through laboratory measurements. But the removal of the existing fluid effects and replacing it by the common fluid (brine) has been achieved through the following steps (Dvorkin, 2003):

In the first stage the effective bulk modulus of pore fluid composition (\bar{K}_{fluid}), is calculated using:

$$\frac{1}{\bar{K}_{fluid}} = \frac{S_{gas}}{K_{gas}} + \frac{S_{oil}}{K_{oil}} + \frac{S_{br}}{K_{br}} \quad (3)$$

where, S_{gas} , S_{oil} , S_{br} , indicate gas, oil and brine saturation and K_{gas} , K_{oil} , K_{br} , correspond to the apparent modulus of gas, oil, and brine. In the next step, bulk modulus of rock (K_{log}), is calculated by equation (4):

$$K_{log} = \rho_b \left(V_p^2 - 4V_s^2 / 3 \right) \quad (4)$$

where, ρ_b is the bulk density and V_p is the compressional wave velocity of the rock. At the next step, bulk modulus of dry rock (K_{dry}) is calculated using the equation (5) and the mineral bulk modulus:

$$K_{dry} = K_{mineral} \frac{1 - (1 - \phi) K_{log} / K_{mineral} - \phi K_{log} / \bar{K}_{fluid}}{1 + \phi - \phi K_{mineral} / \bar{K}_{fluid} - K_{log} / K_{mineral}} \quad (5)$$

where, ϕ is porosity and $K_{mineral}$ is the apparent modulus in the mineral phase (Thomsen, 1986). The bulk modulus of rock saturated with brine (K_{common}) is determined by:

$$K_{common} = K_{mineral} \frac{\phi K_{dry} - (1 + \phi) K_{cf} K_{dry} / K_{mineral} + K_{cf}}{(1 - \phi) K_{cf} + \phi K_{mineral} - K_{cf} K_{dry} / K_{mineral}} \quad (6)$$

where, K_{cf} is the bulk modulus. The compressional wave modulus of the rock saturated with brine (M_{common}) is calculated using the following formula:

$$M_{common} = K_{common} + \rho_b 4V_s^2 / 3 \quad (7)$$

The compressional wave velocity after removal of the primary fluid and replacing it with brine is obtained by:

$$V_p' = \sqrt{M_{common} / \rho_b} \quad (8)$$

In this case, when the shear wave data is not available, compressional wave modulus (M_{log}) is calculated from charts (logs) using the following relation:

$$M_{log} = \rho_b V_p^2 \quad (9)$$

The compressional wave modulus of the dry rock (M_{dry}) is also calculated using compressional wave modulus of the rock's minerals:

$$M_{dry} = M_{mineral} \frac{1 - (1 - \phi) M_{log} / M_{mineral} - \phi M_{log} / \bar{K}_{fluid}}{1 + \phi - \phi M_{mineral} / \bar{K}_{fluid} - M_{log} / K_{mineral}} \quad (10)$$

$$M_{mineral} = K_{mineral} + 4\mu_{mineral} / 3 \quad (11)$$

where, ϕ is porosity, $\mu_{mineral}$ is shear modulus and $K_{mineral}$ is the apparent modulus in the mineral phase. The changes in the elastic modules of different minerals as a whole have been estimated (Takahashi, 2005). Finally, the compressional wave modulus of the brine saturated rock (M_{common}) is calculated as follows:

$$M_{common} = M_{mineral} \frac{\phi M_{dry} - (1 + \phi) K_{cf} M_{dry} / M_{mineral} + K_{cf}}{(1 - \phi) K_{cf} + \phi M_{mineral} - K_{cf} M_{dry} / K_{mineral}} \quad (12)$$

Greenberg - Castagna formula is defined for rocks completely saturated with brine. In this paper, the apparent modulus (K_{cf}) of 2/25 is assumed for brine saturated cases.

It is worth mentioning that the fluid changes have no effect on shear wave modulus, which is the same before and after complete saturation with brine.

2.2 Estimating Geomechanical parameters

Here to determine the bulk modulus, shear modulus, and Young's modulus of rocks, we assumed that they are elastic, homogeneous and isotropic and used the following formula:

$$K = \rho \left(V_p^2 - \left(\frac{4}{3} \right) V_s^2 \right) \quad (13)$$

$$G = \rho \times V_s^2 \quad (14)$$

$$E = \rho \times V_s^2 \times \frac{3V_p^2 - 4V_s^2}{V_p^2 - V_s^2} \quad (15)$$

3 Laboratory Set up and Measurements

The data used in this study were collected by a core flooding system at the laboratory of petroleum engineering department, Curtin University of Technology, Australia. The tested sandstone sample has the volume of 2.350 (gr/cm³), 3.79 cm in diameter, 7.98 cm in length and the porosity of 36/43 deg. After drying and preliminary preparation of this sample, it was placed in a polymer sleeve to be protected from the fluid axial pressure applied. The sample was placed inside the core holder, and piezoelectric (transducers) were placed on the caps to send and receive the acoustic wave. Figure 2 shows schematically, how the sample and exposure transducer were placed.

As seen in Figure 2, the enclosed sample is under P_r pressure (radial pressure) and axial pressure, P_{ax} , is applied. In these conditions, the pore pressure is shown as P_p . In Figure 2, OD represents the outside diameter of the cap, ID represents the inside diameter of the cap, r is the core radius and P_{axial} is effective axial pressure that is calculated as in equation (16):

$$\left. \begin{aligned} A_1 &= \left(\pi (OD)^2 - \pi (ID)^2 \right) \\ A_2 &= \pi r^2 \end{aligned} \right\} \longrightarrow \sigma = P_{axial} = P_{ax} * A_1 / A_2 \quad (16)$$

Different parts of this chamber which is in direct contact with the fluid, are neutral to chemical reaction. At the ends of this chamber, two caps are placed where the transducers have been installed. As seen in Figure 3, the receiver and transmitter are in direct contact with the sample.

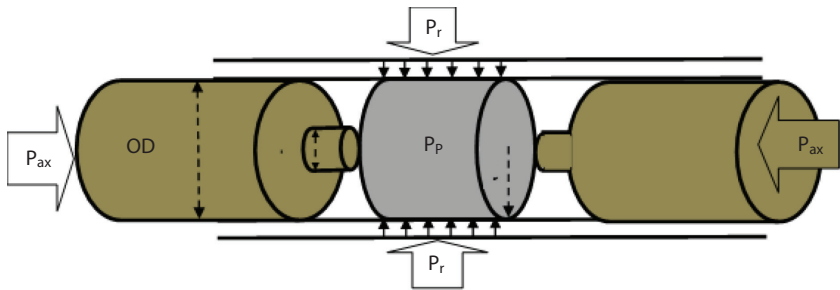


Figure 2 The placement of the test device is shown in schematic form.

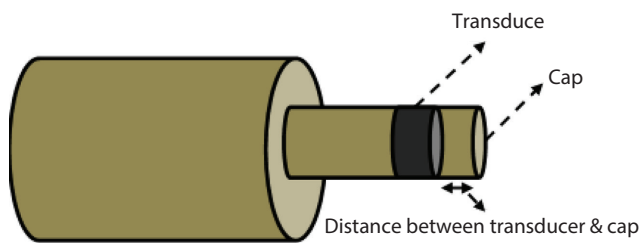


Figure 3 Schematic, placement of sample with transducer and the top cap.

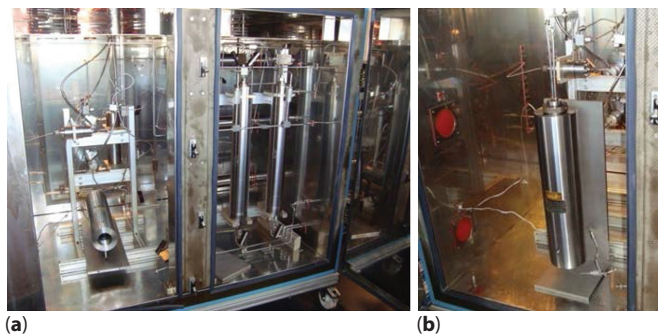


Figure 4 (a) The core flooding system, (b) Image of the holder connected to the core and transducers.

The laboratory system is equipped with a back pressure regulator (BPR), to make it possible to simulate the behavior of real reservoir pressure. For axial and confining pressures, a hand pump has been used, and to achieve pore pressure, a hydraulic pump has been utilized. This test has been performed at room temperature. Signals are stored in a computer equipped with particular software which has the capability to integrate into the oscilloscope. Shown in Figure 4a is the complete flooding system device with three different fluid injection capsule, each with different kinds of fluids and the oven chamber that maintains the desired test temperature (46 °C in this experiment). Figure 4b indicates a picture of the core holder and connected transducers.

It should be noted that the injected fluid in this experiment is CO₂ supercritical, which has been injected under 1300 psi pressure and a temperature of 46 °C at a rate of 1 (ml/min) into the sample saturated with distilled water.

1.3 Laboratory Data Collection

Travel times of compressional and shear waves through the super critically CO₂ saturated core sample were measured at six different effective pressures (within

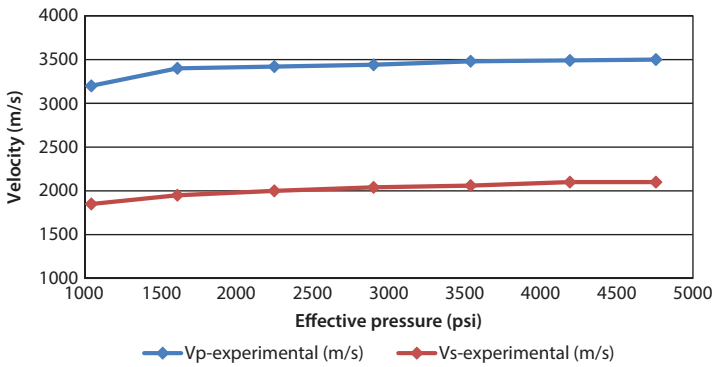


Figure 5 Compressional and shear wave velocity vs different effective pressure for super critically saturated core sample.

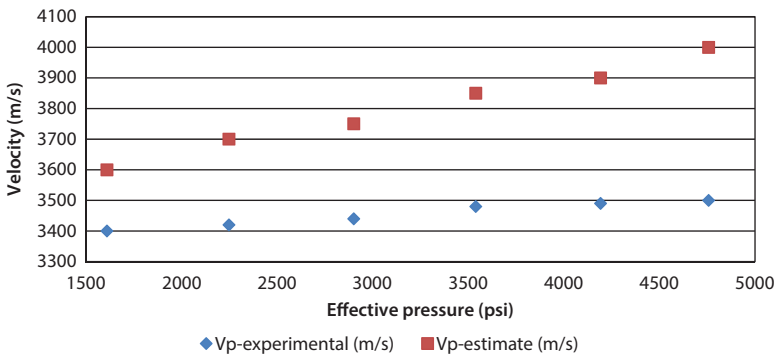


Figure 6 P-wave velocity (experimental and estimated) at different effective pressures.

the reservoir pressure range). Later on, corresponding compressional and shear wave velocities were calculated (Figure 5).

4 Results and Discussion

To see how closely estimated wave velocity correlates with the experimental velocity values; we replaced the primary CO_2 saturated water with brine (using apparent module of 2.25) using Gassmann equation. Then using the Greenberg-Castagna formula we estimated the compressional wave velocity (Figure 6).

In Figure 6, the compressional wave velocity obtained from the laboratory experiment and the Gassmann equation is depicted versus effective pressure. It can be noticed that at all effective pressures the estimated velocities have higher values than experimental ones. The difference gradually enlarges as the effective pressure is increased. The rate of velocity increment is faster for estimated velocity

than the experimental counterpart. This is because in Gassmann theory environment (the core) is considered a homogeneous and isotropic elastic environment. This theory is often true for Monomineralic rocks such as pure quartz sandstone or clean limestone. But since the sample used in this study developed naturally, possible impurities exist such as clay or fine cracks; so wave scattering is not considered in the Gassmann equations. It is also effective on bulk modulus and often in this hypothesis, it is assumed to be average. Another issue to the assumptions of this model is the fluid replacement instead of several fluids, regardless of their distribution in the environment and is often considered to be the average of the density of the fluids. This is effective on the accuracy of the model especially while the saturation is not uniform (Patchy saturation). Also with the pressure increasing, joints and cracks closed more and reduced permeability. Therefore, fluid flow and the opportunity to achieve balance are much reduced and the operating result is that Gassmann theory pushes farther than expected.

Shear wave velocity of the rock sample was determined at the different pressure from the estimated compressional wave velocity, using Greenberg-Castagna formulas.

Figure 7 shows the experimental and estimated shear wave velocity values at different effective pressures. As it can be seen in contrary to the compressional wave, the estimated shear wave velocity is very much in accordance with the corresponding experimental values. Particularly this compatibility is more obvious at low effective pressures. The difference between experimental and estimated velocities and the rate of changes increase as the applied pressure increases. This is because the shear waves are only sensitive to changes solid in the environment. With the increase in effective pressure and reduced porosity and micro cracks, stone resistance increases against deformation (while volume or angle); as a result, it will face increasing shear wave velocity. Since in Greenberg- Castagna equation compressional and shear wave communication waves can be described with porosity and modules, effective stress plays

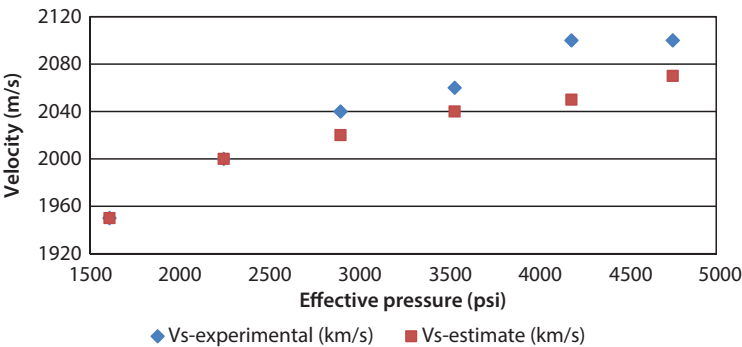


Figure 7 S-wave velocity (experimental and estimated) at different effective pressures.

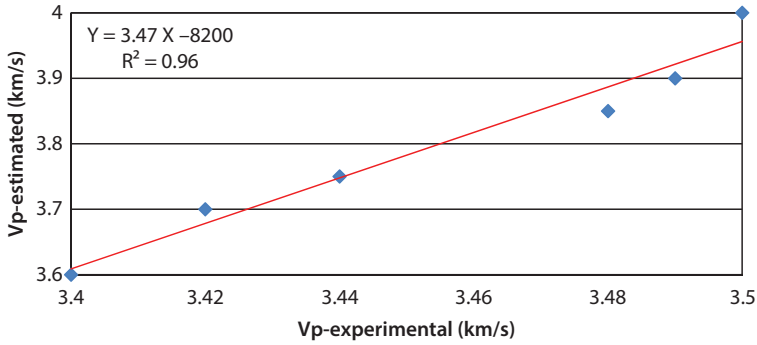


Figure 8 Cross plot of estimated P-wave velocities vs. laboratory measurements.

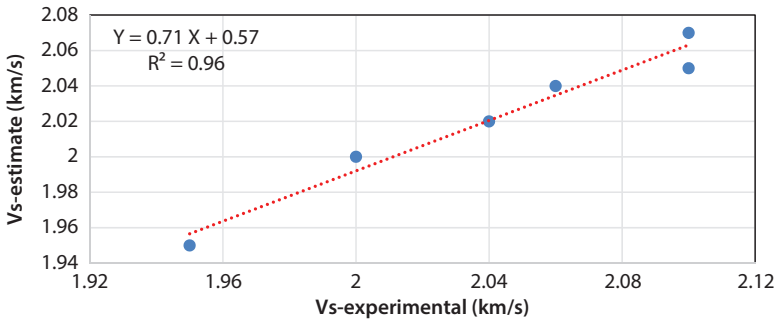


Figure 9 Cross plot of the estimated S-wave velocities vs. laboratory measurements.

an important role in the trend of estimation. But because of unconsidered pore shape, form, size, and density of fractures, anisotropy, texture and especially effective pressure on the environment in this relationship, differences although small can be seen in the results.

Figure 8 shows cross plot of the compressional wave velocity measured in the laboratory condition vs. the estimated values along with a best-fitted line. The correlation of the values is 0.95. Figure 9 also shows the cross plot of the experimental and estimated shear wave velocities along with a best fitted line. The correlation of the values is 0.96.

$$V_{P(Estimate)} = 3.47 V_{P(Experimental)} - 8200 \text{ (km/s)}$$

$$R^2 = 0.96$$

$$V_{S(Estimate)} = 0.71 V_{S(Experimental)} + 0.57 \text{ (km/s)}$$

$$R^2 = 0.96$$

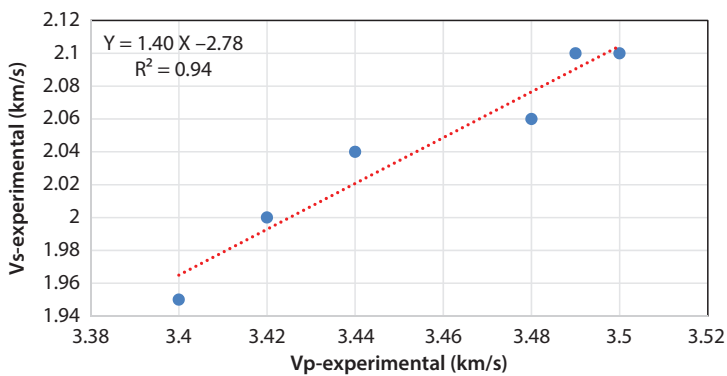


Figure 10 Plot of experimental shear wave velocity against compressional wave velocity.

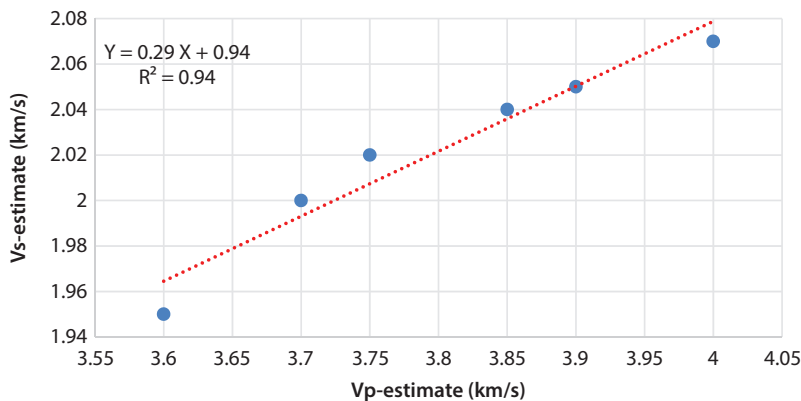


Figure 11 Plot of estimated shear wave velocity against compressional wave velocity.

Figures 10 and 11 show the cross plots of the experimental and estimated compressional and shear wave velocities. Mathematical relationship between two sets of wave velocities were obtained. As it shows 90% correlation observed in both modes between compressional and shear wave velocity. The important note is that the slope of the curve is approximately 5 times in the experimental measurements more than the estimated measurement and this is due to larger estimated compressional wave velocity.

Since Greenberg- Castagna model assumptions is ideal for a specially designed environment, there is no great match between this model and laboratory values. But as was mentioned earlier, correspondence between the velocity, the pressure and shear are very close together. It seems environment effective pressure is the essential factor that change is not considered in the model. This effect is highlighted on shear wave velocity and shear wave module.

$$\begin{aligned}
 V_{S(\text{Greenberg} - \text{Castagna})} &= 0.86V_{P(\text{Greenberg} - \text{Castagna})} + 1.17 \\
 V_{S(\text{Experimental})} &= 1.40V_{P(\text{Experimental})} - 2.78 \text{ (km/s)} \\
 R^2 &= 0.94 \\
 V_{S(\text{Estimate})} &= 0.29V_{P(\text{Estimate})} + 9.4 \text{ (km/s)} \\
 R^2 &= 0.94
 \end{aligned}$$

As it can be seen in Figure 12, the behavior of Vs-Experimental/estimated are almost independent of variability of effective pressure. While VP-Experimental/estimated increases with the rising effective pressure. The difference between rates of VP's is because of some assumptions of Gassmann-Greenberg-Castagna equations, which they guess that media is ideal.

At this stage, we compared the elastic coefficients of rock samples obtained from experimental velocity values, and those estimated from Greenberg-Castagna model. According to Figure 13, the correlation between experimental and estimated values for volume or bulk modulus is very low and is about 0.1. This is because the compressibility of the pores media depends on the minerals type and texture of the rock. Also, it is a function of the amount and shape of media porosity. When the pores are filled with fluid, elastic modulus is affected by many parameters of fluid such as the compressibility, the kind of fluid, distribution, viscosity and also fluid incompressibility.

The fluid used in this study has a patchy saturation and has created anisotropic, heterogeneous environments. Besides that, different effective pressures

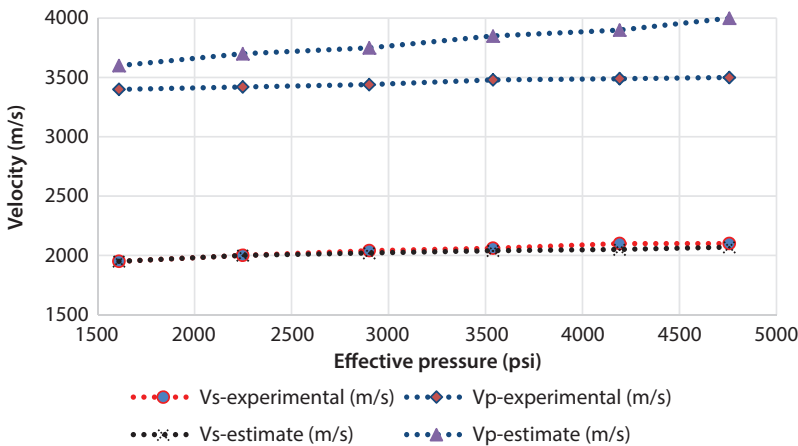


Figure 12 Rate of variability of experimental/estimated velocities with increasing effective pressure.

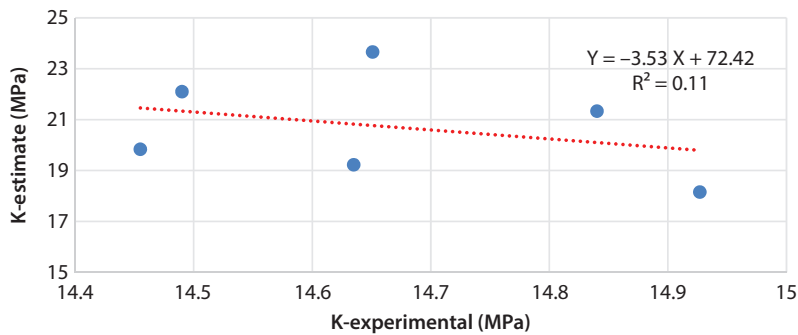


Figure 13 Plot of Laboratory vs. estimated Bulk modulus (K) of rock sample.

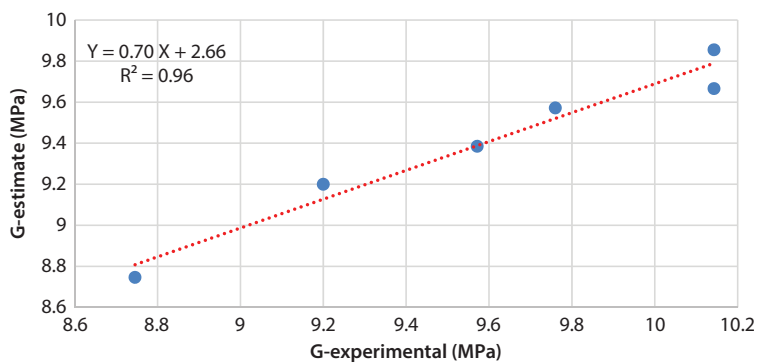


Figure 14 Plot of laboratory vs. estimated shear modulus.

that applied on a frame stone, impressed the results of Gassmann - Greenberg – Castagna equations.

$$K_{(Estimate)} = -3.53K_{(Experimental)} + 72.42 \text{ (MPa)}$$
$$R^2 = 0.11$$

One of the assumptions of Gassmann equations is that the shear modulus in the dry and wet state is constant. It seems that this assumption is not applicable for most environments. The fact is that the changes to the texture of rock due to the reaction between rock and the fluid cause a change in the shear modulus of saturated rocks. Changes in the shear modulus is the main cause for the difference between the experimental velocity and the calculated velocity utilizing the Gassmann equations. Anyway, these differences in shear modulus cause a decrease in the use of Gassmann theory to estimate the velocity. These differences can be observed in Figure 14 for both laboratory and estimated values. Although the correlation

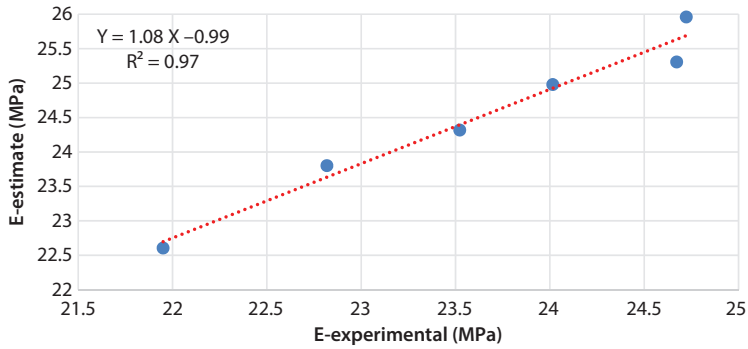


Figure 15 Plot of laboratory vs. estimated Young's modulus.

between experimental and estimated values are very high and close to 0.96, by replacing the common fluid and use of the estimated shear wave velocity, shear modulus values change a little as well. The reason behind this phenomenon is the defect in the Gassmann hypothesis that the shear modulus for rock is equal in both dry and saturated conditions. The reaction between the fluid and the texture of the rock is consequently causing a change in the shear modulus of saturated rocks.

$$G_{(Estimate)} = 0.70G_{(Experimental)} + 2.66 \text{ (MPa)}$$

$$R^2 = 0.96$$

But based on the values in Figure 15, the experimental and the estimated values of Young's modulus are very close to one another and very comparable (%97).

$$E_{(Estimate)} = 1.08E_{(Experimental)} - 0.99 \text{ (MPa)}$$

$$R^2 = 0.97$$

5 Conclusions

In this paper we evaluated the closeness of the estimated elastic wave velocities and elastic modulus of a rock sample via Gassmann - Greenberg - Castagna formula to those obtained from laboratory measurements at reservoir pressure.

- Estimating the physical parameters of rock samples from Gassmann - Greenberg - Castagna equations at high pressures is farther from the real situation. At high pressure, velocity values are more differentiated from each other and the estimated values are observed to be very far from the experimental (laboratory) values. Although it appears that at higher pressures cracks or fractures get closed, in substituting the fluid, especially brine for supercritical carbon dioxide and water, elasticity values have very

high variations, and this very strongly influences the estimated compression wave velocities. And finally, this effect can be seen on the shear wave derived from compression wave. But since the shear wave velocity in the fluid and gas behave similarly, the effect was observed less on this wave.

- In the Gassmann assumptions it has been stated that pore fluid will not modify the elastic properties of the rocks. Thus, this theory predicts that shear modulus is not affected by the fluid saturation and will remain constant. In this study, the shear modulus didn't remain constant during fluid saturation and during the transformation from gas- water saturation state to water saturation state; changes were detected to be around 2 percent. Because of this change in the shear modulus, it makes one hesitate to utilize the Gassmann theory to calculate the velocity. With the calculated and the experimental values of the shear modulus being variable, it can be concluded that Gassmann theory is not accurate for estimating the compressional wave velocity in a saturated state.
- The research found that the bulk modulus values obtained from the laboratory experiments show a very weak compatibility with the values calculated using Gassmann formulas. One of the probable reasons for this could be an influence of the transformation of the rock skeleton by brine (salt water). The overall conclusion from these studies is that, for samples saturated in brine at low pressures, good agreement exists between bulk modulus values calculated from Gassmann formula and experimental values obtained in the laboratory. While at high pressures when the rock is very strongly influenced by pressure, this agreement is nonexistent. This change was about 9% at low pressures and at high pressures, these differences reached up to 23%. Therefore, one should contemplate before utilizing Gassmann equation.

6 Acknowledgment

Authors extended their appreciation to Petroleum Engineering Department, Curtin University of Technology, Australia that provided the authors the opportunity to utilize the laboratory core flooding system. Also, the authors thank and appreciate very much Prof. Vamegh Rasouli, Dr. Amin Nabipour, Dr. Mohammad Sarmadi and Dr. Mohsen Ghasemi for their help in conducting these experiments. Finally, the authors are very grateful and extend their deepest appreciation to the respected faculty of Petroleum Engineering and Geophysics departments, Curtin University of Technology that cooperated in the design, manufacturing and installation of the transducers.

References

- P. Avseth, T. Mukerji, and G. Mavko, *Quantitative Seismic Interpretation*, Cambridge University Press, Cambridge (2005). F. G. Bell, *Engineering Properties of Soil and Rocks*, 4th ed., Back well science Ltd, United Kingdom (2000).

DOI: 10.7569/JSEE.2017.629502

- J. P. Castagna, M. L. Batzle, and R. L. Eastwood, Relationship between compressional and shear wave velocities in silicate rocks. *Geophysics* **50**, 571–581 (1985).
- M. A. Dezfouli, Body wave velocities estimation from wireline log data utilizing an artificial neural network for a carbonate reservoir, South Iran. *J. Petrol. Sci. Technol.* **31**(1), 32–43 (2013).
- S. N. Domenico, Rock lithology and porosity determination from shear and compressional velocity. *Geophysics* **49**, 1188–1195 (1984).
- J. P. Dvorkin, and S. Alkhater, Pore fluid and porosity mapping from seismic, *First Break*, **22**, 53–57 (2004).
- D. Eberhart, Ph., Investigation of crustal structure and active tectonic processes in the coast ranges, central California, PhD. thesis in Stanford University (1989).
- A. J. Engel and G. R. Bashford, A new method for shear wave speed estimation in shear wave elastography. *IEEE T. Ultrason. Ferr.* **62**(12), 2016–2114.
- F. Gassmann, On the elasticity of porous media: Vierteljahrsschrift der Naturforschenden Gesellschaft in Zurich. **96**, 1–23 (1951).
- M. L. Greenberg and J. P. Castagna, Shear wave velocity estimation in porous rocks: Theoretical formulation, preliminary verification and applications, *Geophysics. Prospecting* **40**, 195–209 (1992).
- J. K. Jang, K. Kondo, T. Namita, M. Yamakawa, and T. Shiina, Comparison of techniques for estimating shear-wave velocity in arterial wall using shear-wave elastography - FEM and phantom study, in IEEE International Ultrasonic Symposium, Taipei, Taiwan, p. 10, (2015).
- D. Han, A. Nur, and D. Morgan, Effects of porosity and clay content on wave velocities in sandstones. *Geophysics* **51**, 2093–2107 (1986).
- D. Han, Empirical relationships among seismic velocity, effective pressure, porosity and clay content in sandstone. *Geophysics* **54**, 82–89 (1989).
- J. S. L. Heurich and M. Long, Correlations between shear wave velocity and geotechnical parameters in Norwegian clays, in *17th Nordic Geotechnical Meeting Challenges in Nordic Geotechnic*, Reykjavik, Iceland, 299–308 (2016).
- M. Krief, J. Garat, J. Stellingwerf, and J. Venter, A petrophysical interpretation using the velocities of P and S waves (full wave from sonic). *Log Anal.* **31**, 35–369 (1990).
- Sh. Malekia, A. Moradzadeh, R. Ghavami Riabi, R. Gholamib, and F. Sadeghzadeh, Prediction of shear wave velocity using empirical correlations and artificial intelligence methods. *RIAG Journal of Astronomy and Geophysics* **3**(1), 70–81 (2014).
- G. Mavko and T. Mukerji, Pore space compressibility and Gassmann's relation. *Geophysics* **60**, 1743–1749 (1995).
- G. Mavko, T. Mukerji, and J. Dvorkin, *Rock Physics Handbook: Tools for Seismic Analysis in Porous Media*, Cambridge University Press, Cambridge (1998).
- P. Milholand, M. H. Manghnani, S. O. Schlanger, and G. H. Sutton, Geoacoustic modeling of deep-sea carbonate sediments. *J. Acoust. Soc. Am.* **68**, 1351–1360 (1980).
- G. R. Pickett, Acoustic character logs and their application in formation evaluation. *J. Petrol. Technol.* **15**, 650–667 (1963).
- M. R. Rezaee, A. Kadkhodaie, and A. Barabadi, Prediction of shear wave velocity from petrophysical data utilizing intelligent systems: An example from a sandstone reservoir of Carnarvon Basin, Australia. *J. Petrol. Sci. Eng.* **55**, 201–212 (2007).
- L. L. Raymer, E. R. Hunt, and J. S. Gardner, An improved sonic transit time-to-porosity transform, Paper P, in *21st Annual Logging Symposium Transactions*, Lafayette, Louisiana (1980).

- J. Raiga-clemenceau, J. P. Martin, and S. Nicoletis, The concept of acoustic formation factor for more accurate porosity determination from sonic transit time data. *The Log Analyst*, Jan-Feb (1988).
- I. Takahashi, Rock physics as a quantitative tool for seismic reservoir characterization, INPEX Corporation, p. 175 (2005).
- L. Thomsen, Weak elastic anisotropy. *Geophys* **51**, 1654–1966 (1986).
- C. Tosaya and A. Nur, Effects of diagenesis and clays on compression velocities in rocks. *Geophysics, Res. Lett.* **9**, 5–8 (1982).
- Z. Wang and A. Nur, *Seismic and Acoustic Velocities in Reservoir Rocks*, Volume 2: SEG Geophysics Reprint Series 10, Society of Exploration Geophysicists (1992).
- B. Widarsono and P. M. Wong, Estimation of rock dynamic elastic property profiles through a combination of soft computing, acoustic velocity modeling, and laboratory dynamic test on core samples, SPE Asia Pacific Oil and Gas Conference, 68712 (2001).
- M. R. J. Wyllie, A. R. Gregory, and L. W. Gardner, Elastic wave velocities in heterogeneous and porous media. *Geophysics* **21**, 41–70 (1956).